

# **Appendix AA**

## **Calibration Documents for Geophones and Agilent 35670A Dynamic Signal Analyzer**

# Calibration Documentation

- 1. 1Hz Geophones (Mark Product)..... AA.3
- 2. 4.5Hz Geophones (Mark Product)..... AA.7
- 3. 4.5Hz Geophones (GeoSpace Product) ..... AA.11
- 4. Dynamic Signal Analyzer (Agilent) ..... AA.15



# Calibration Procedure: Mark Products L4 Geophones

Performed: October 19, 2007

Expires: October 19, 2008

## 1. Equipment Calibrated Using This Procedure:

EQUIPMENT	DESCRIPTION	SERIAL NUMBER
Mark Products L4	Geophones	3770, 3773, 3774, 3775

## 2. NIST Traceable Reference Equipment Used in Calibration:

EQUIPMENT	DESCRIPTION	SERIAL NUMBER	CALIBRATION #	CAL. DATE	EXP. DATE
Agilent 34401A	Digital Multimeter	US36105870	006846	7/16/2007	7/16/2008
Columbia	Accelerometer 3021	2120	998953	8/08/2007	8/08/2008
Columbia	Charge Amplifier 4102M	813	998954	8/08/2007	8/08/2008
Agilent 35670A	Dynamic Signal Analyzer	MY41005676	002104	4/16/2007	4/16/2008

## 3. Other Previously Verified Equipment Used in Calibration:

EQUIPMENT	DESCRIPTION	SERIAL NUMBER	CAL. DATE	EXP. DATE
Bently-Nevada	19049 Proximitator	120137	10/18/2007	10/18/2008

Performed by : MinJae Jung

Verified by : WonKyoung Choi

Checked by : Kenneth H. Stokoe II

Date : October 19, 2007

# Mark Products L-4 Geophone Calibration – 19 October 2007

Calibration Date : 10/19/2007

Expiration Date : 10/19/2008

Performed by Min Jae Jung

(Limited Calibration : Phase Only)

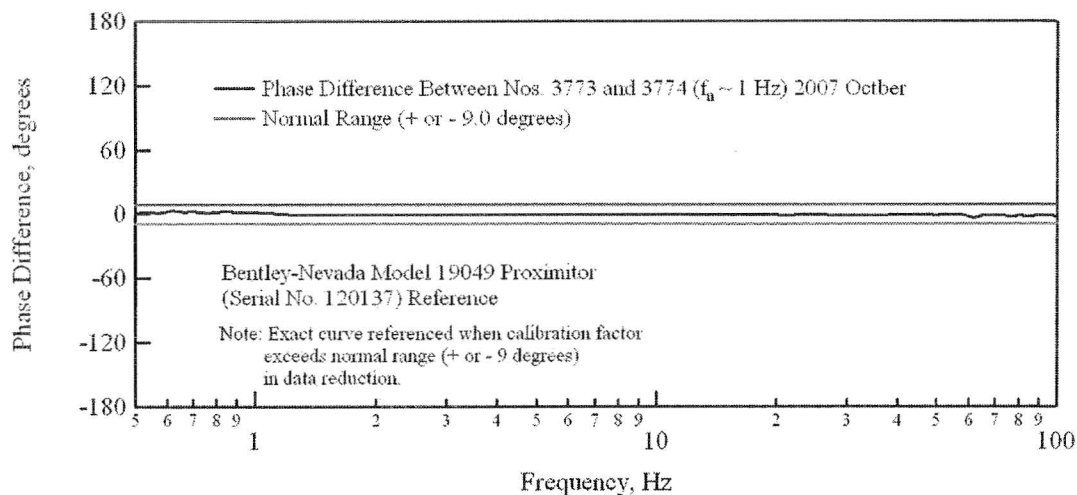


Figure AA1 Phase Difference Between Mark Products L4 Geophones 3773 and 3774, 1- Hz Resonant Frequency; Calibrated Relative to Bently-Nevada Model 19049 Proximitors (Serial No. 120137)- 19 October 2007

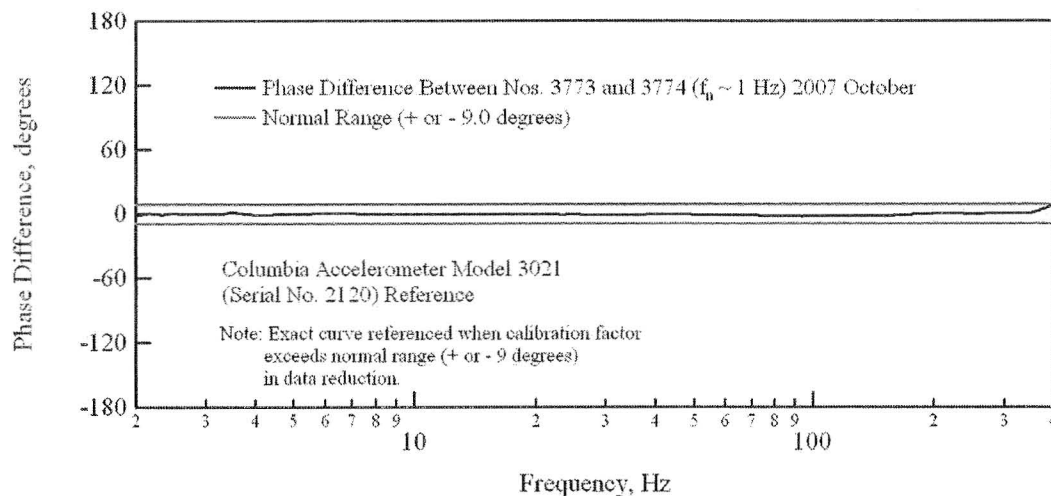


Figure AA2 Phase Difference Between Mark Products L4 Geophones 3773 and 3774, 1- Hz Resonant Frequency; Calibrated Relative to Columbia Accelerometer Model 3021 (Serial No. 2120)- 19 October 2007

# Mark Products L-4 Geophone Calibration – 19 October 2007

Calibration Date : 10/19/2007

Expiration Date : 10/19/2008

Performed by Min Jae Jung

(Limited Calibration : Phase Only)

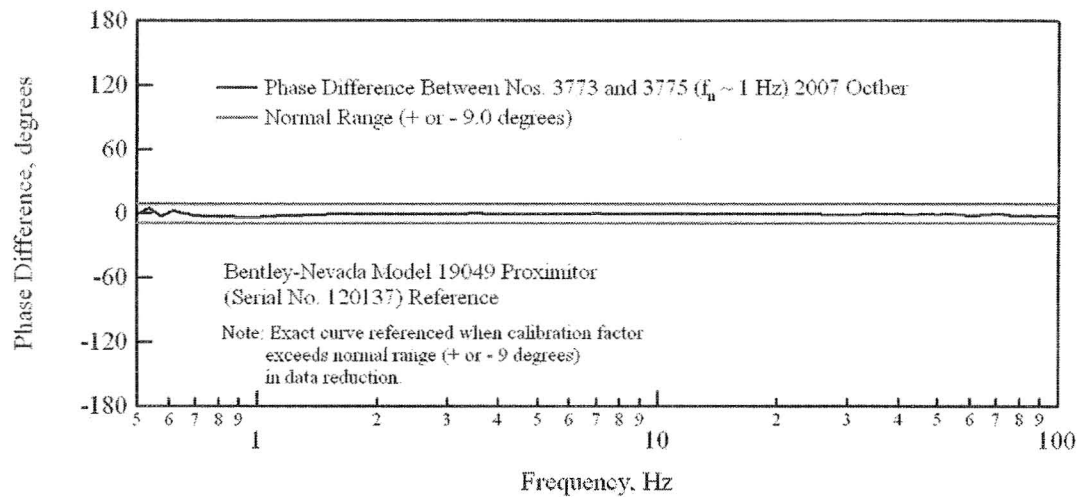


Figure AA3 Phase Difference Between Mark Products L4 Geophones 3773 and 3775, 1- Hz Resonant Frequency; Calibrated Relative to Bentley-Nevada Model 19049 Proximitors (Serial No. 120137)- 19 October 2007

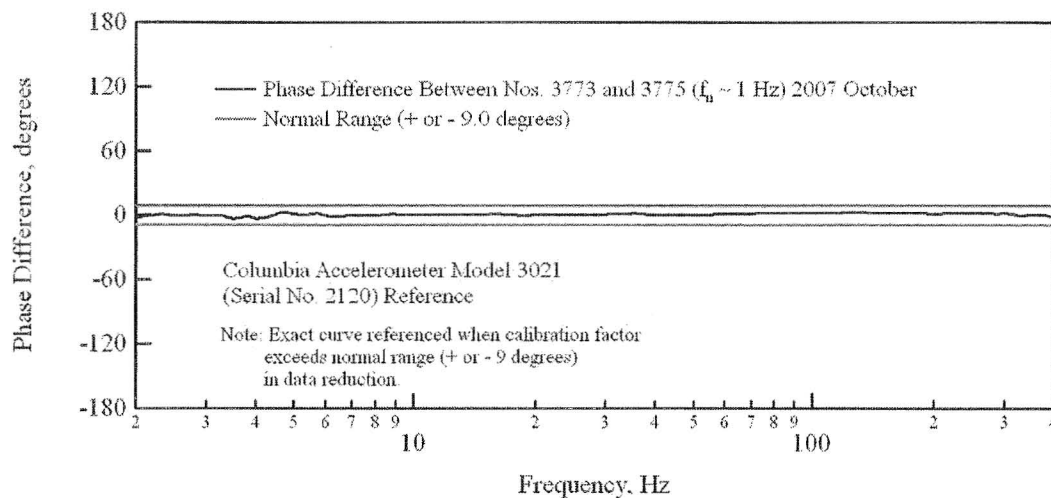


Figure AA4 Phase Difference Between Mark Products L4 Geophones 3773 and 3775, 1- Hz Resonant Frequency; Calibrated Relative to Columbia Accelerometer Model 3021 (Serial No. 2120)- 19 October 2007

**Mark Products L-4 Geophone Calibration – 19 October 2007**

Calibration Date : 10/19/2007

Expiration Date : 10/19/2008

Performed by Min Jae Jung

(Limited Calibration : Phase Only)

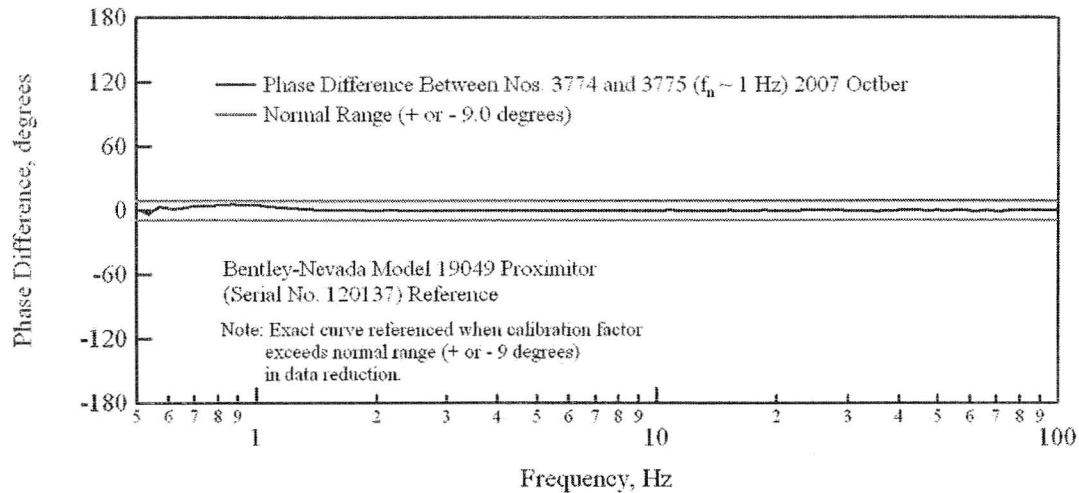


Figure AA5 Phase Difference Between Mark Products L4 Geophones 3774 and 3775, 1- Hz Resonant Frequency; Calibrated Relative to Bently-Nevada Model 19049 Proximitors (Serial No. 120137)- 19 October 2007

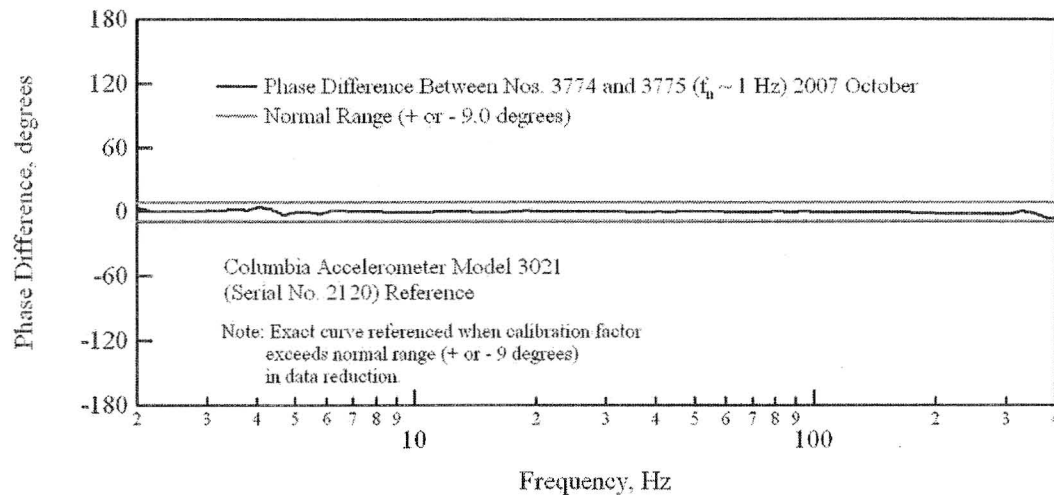


Figure AA6 Phase Difference Between Mark Products L4 Geophones 3774 and 3775, 1- Hz Resonant Frequency; Calibrated Relative to Columbia Accelerometer Model 3021 (Serial No. 2120)- 19 October 2007

# Calibration Procedure: Mark Products L10

## Geophones

Performed: October 19, 2007

Expires: October 19, 2008

### 1. Equipment Calibrated Using This Procedure:

EQUIPMENT	DESCRIPTION	SERIAL NUMBER
Mark Products L10	Geophones	92001, 92002, 92003

### 2. NIST Traceable Reference Equipment Used in Calibration:

EQUIPMENT	DESCRIPTION	SERIAL NUMBER	CALIBRATION #	CAL. DATE	EXP. DATE
Agilent 34401A	Digital Multimeter	US36105870	006846	7/16/2007	7/16/2008
Columbia	Accelerometer 3021	2120	998953	8/08/2007	8/08/2008
Columbia	Charge Amplifier 4102M	813	998954	8/08/2007	8/08/2008
Agilent 35670A	Dynamic Signal Analyzer	MY41005676	002104	4/16/2007	4/16/2008

### 3. Other Previously Verified Equipment Used in Calibration:

EQUIPMENT	DESCRIPTION	SERIAL NUMBER	CAL. DATE	EXP. DATE
Bently-Nevada	19049 Proximitator	120137	8/14/2006	8/14/2007

Performed by : MinJae Jung

Verified by : WonKyoung Choi

Checked by : Kenneth H. Stokoe II

Date : October 19, 2007

# **Mark Products L-10 Geophone Calibration – 19 October 2007**

Calibration Date : 10/19/2007

Expiration Date : 10/19/2008

Performed by Min Jae Jung

(Limited Calibration : Phase Only)

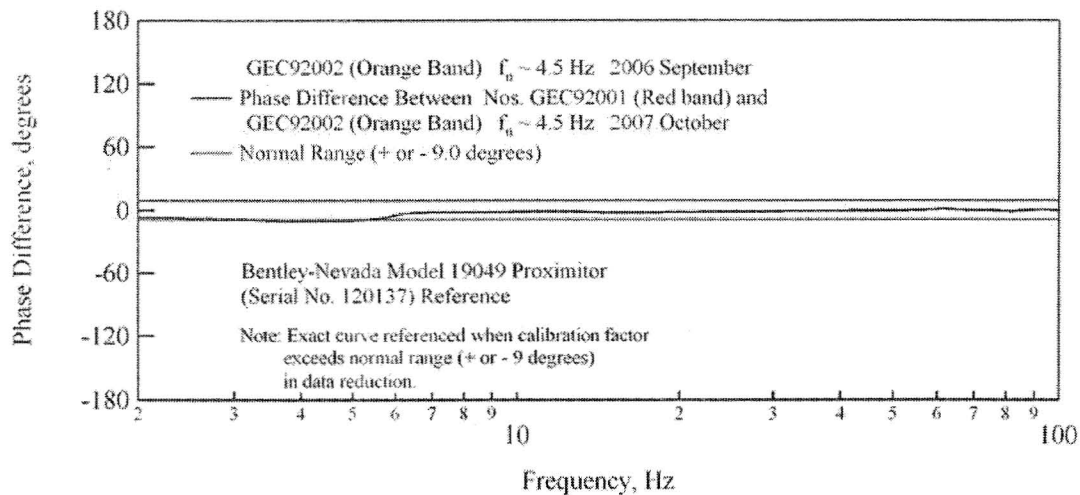


Figure AA7 Phase Difference Between Mark Products L10 Geophones 92001 and 92002, 4.5-Hz Resonant Frequency; Calibrated Relative to Bentley-Nevada Model 19049 Proximitors (Serial No. 120137)- 19 October 2007

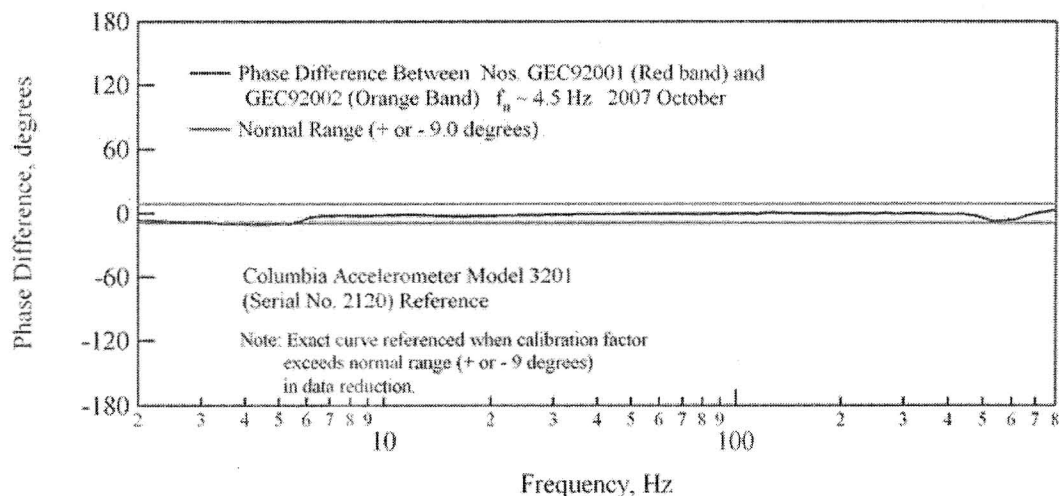


Figure AA8 Phase Difference Between Mark Products L10 Geophones 92001 and 92002, 4.5-Hz Resonant Frequency; Calibrated Relative to Columbia Accelerometer Model 3021 (Serial No. 2120)- 19 October 2007

# **Mark Products L-10 Geophone Calibration – 19 October 2007**

Calibration Date : 10/19/2007

Expiration Date : 10/19/2008

Performed by Min Jae Jung

(Limited Calibration : Phase Only)

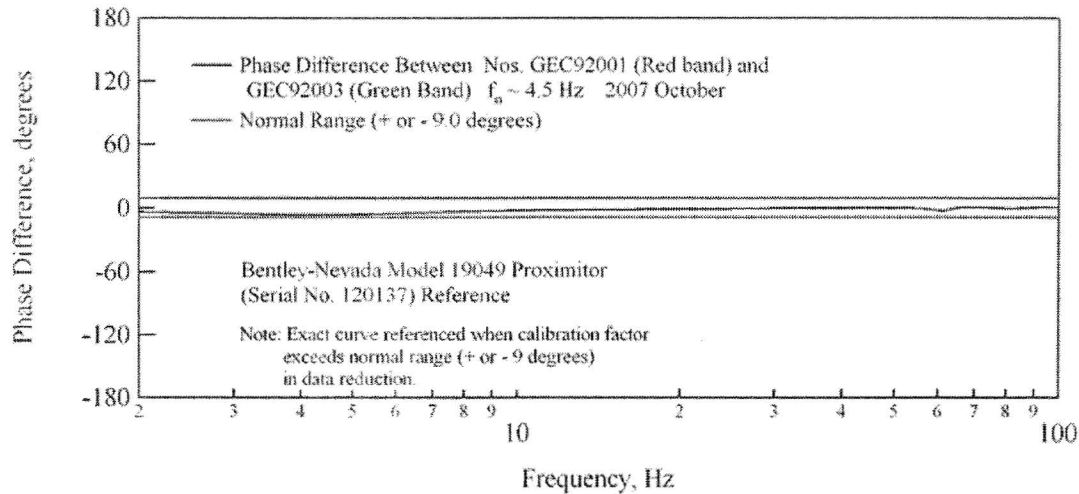


Figure AA9 Phase Difference Between Mark Products L10 Geophones 92001 and 92003, 4.5-Hz Resonant Frequency; Calibrated Relative to Bentley-Nevada Model 19049 Proximitors (Serial No. 120137)- 19 October 2007

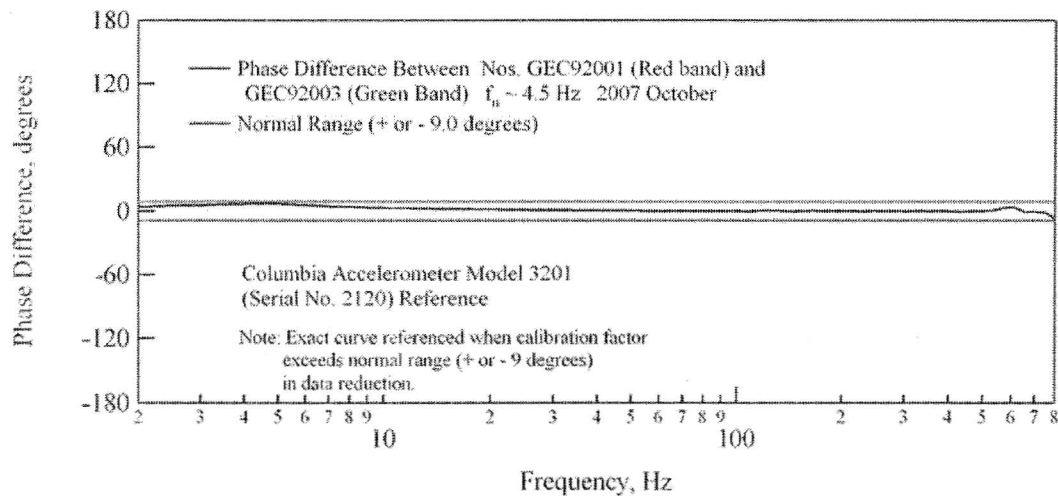


Figure AA10 Phase Difference Between Mark Products L10 Geophones 92001 and 92003, 4.5-Hz Resonant Frequency; Calibrated Relative to Columbia Accelerometer Model 3021 (Serial No. 2120)- 19 October 2007

# Mark Products L-10 Geophone Calibration – 19 October 2007

Calibration Date : 10/19/2007

Expiration Date : 10/19/2008

Performed by Min Jae Jung

(Limited Calibration : Phase Only)

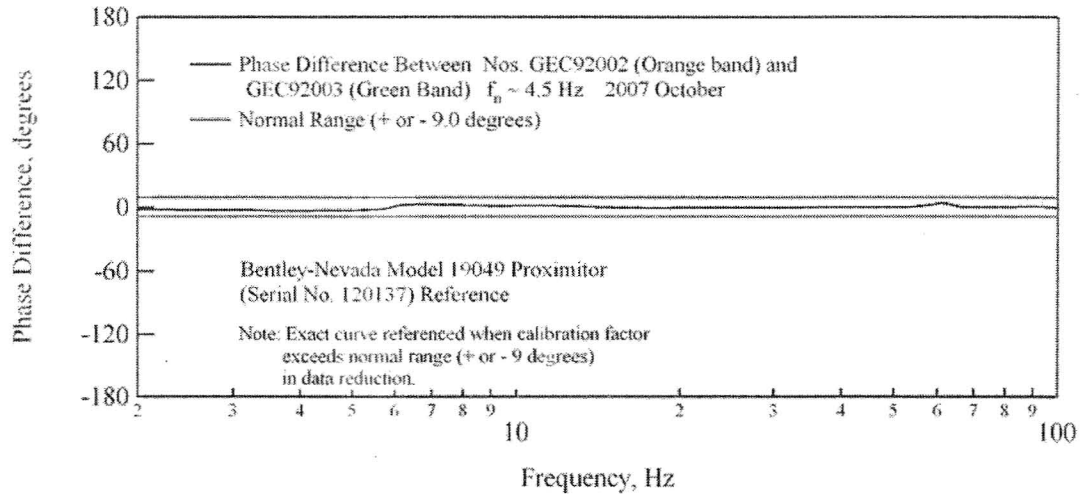


Figure AA11 Phase Difference Between Mark Products L10 Geophones 92002 and 92003, 4.5-Hz Resonant Frequency; Calibrated Relative to Bentley-Nevada Model 19049 Proximator (Serial No. 120137)- 19 October 2007

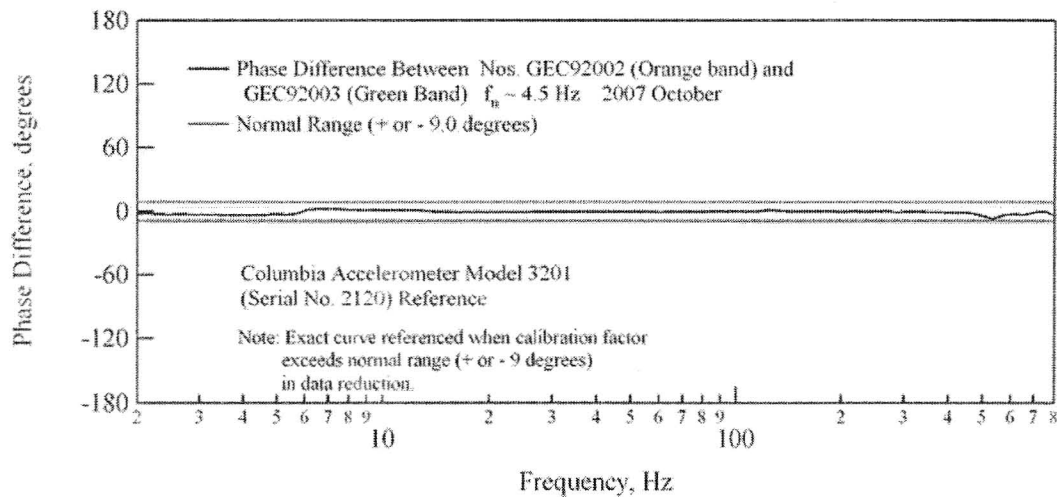


Figure AA12 Phase Difference Between Mark Products L10 Geophones 92002 and 92003, 4.5-Hz Resonant Frequency; Calibrated Relative to Columbia Accelerometer Model 3021 (Serial No. 2120)- 19 October 2007



# Calibration Procedure: Geo Space GS-11D Geophones

Performed: December 07, 2007

Expires: December 07, 2008

## 1. Equipment Calibrated Using This Procedure:

EQUIPMENT	DESCRIPTION	SERIAL NUMBER
Geo Space GS-11D	Geophones	UT07-4.5Hz-02
		UT07-4.5Hz-03
		UT07-4.5Hz-04

## 2. NIST Traceable Reference Equipment Used in Calibration:

EQUIPMENT	DESCRIPTION	SERIAL NUMBER	CALIBRATION #	CAL. DATE	EXP. DATE
Agilent 34401A	Digital Multimeter	US36105870	006846	7/16/2007	7/16/2008
Columbia	Accelerometer 3021	2120	998953	8/08/2007	8/08/2008
Columbia	Charge Amplifier 4102M	813	998954	8/08/2007	8/08/2008
Agilent 35670A	Dynamic Signal Analyzer	MY41005676	002104	4/16/2007	4/16/2008

## 3. Other Previously Verified Equipment Used in Calibration:

EQUIPMENT	DESCRIPTION	SERIAL NUMBER	CAL. DATE	EXP. DATE
Bently-Nevada	19049 Proximitior	120137	10/18/2007	10/18/2008

Performed by : Jiabei Yuan

Verified by : MinJae Jung

Checked by : Kenneth H. Stokoe II

Date : December 07, 2007

# **GeoSpace GS-11D Geophone Calibration – 07 December 2007**

Calibration Date : 12/07/2007

Expiration Date : 12/07/2008

Performed by : Jiabei Yuan

(Limited Calibration : Phase Only)

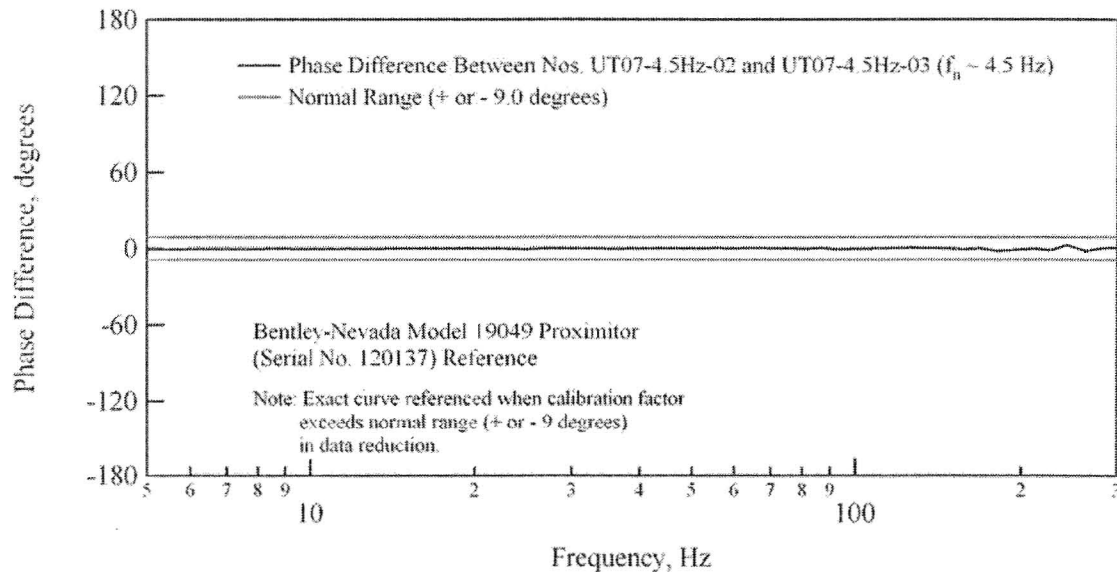


Figure AA13 Phase Difference Between GeoSpace GS-11D Geophones UT07-4.5Hz-02 and UT07-4.5Hz-03, 4.5 - Hz Resonant Frequency; Calibrated Relative to Bentley-Nevada Model 19049 Proximitor (Serial No. 120137) - 07 December 2007

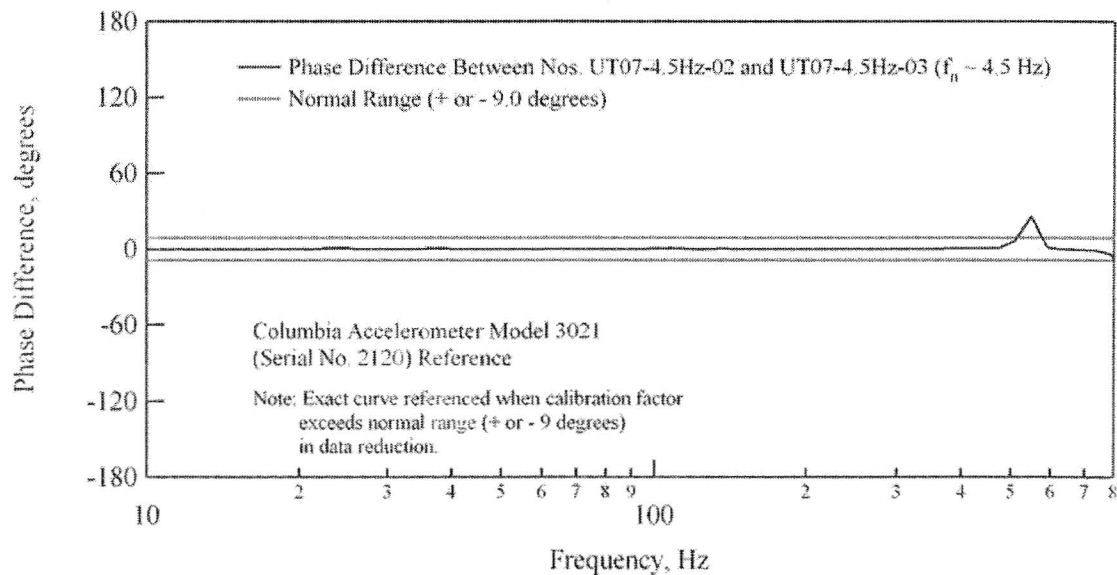


Figure AA14 Phase Difference Between GeoSpace GS-11D Geophones UT07-4.5Hz-02 and UT07-4.5Hz-03, 4.5 - Hz Resonant Frequency; Calibrated Relative to Columbia Accelerometer Model 3021 (Serial No. 2120) - 07 December 2007

# GeoSpace GS-11D Geophone Calibration – 07 December 2007

Calibration Date : 12/07/2007

Expiration Date : 12/07/2008

Performed by : Jiabei Yuan

(Limited Calibration : Phase Only)

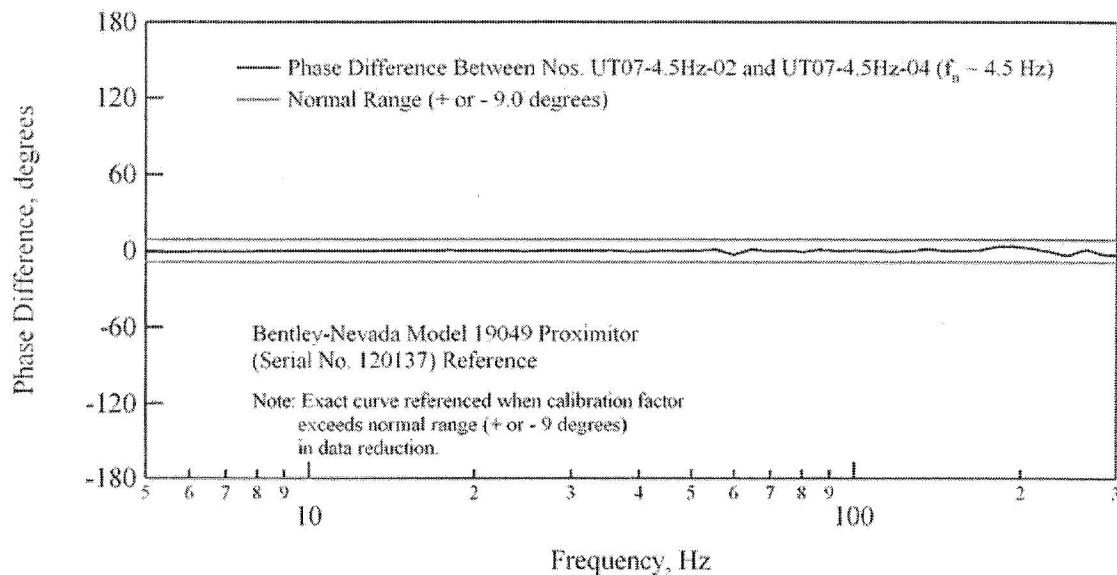


Figure AA15 Phase Difference Between GeoSpace GS-11D Geophones UT07-4.5Hz-02 and UT07-4.5Hz-04, 4.5 - Hz Resonant Frequency; Calibrated Relative to Bentley-Nevada Model 19049 Proximitors (Serial No. 120137) - 07 December 2007

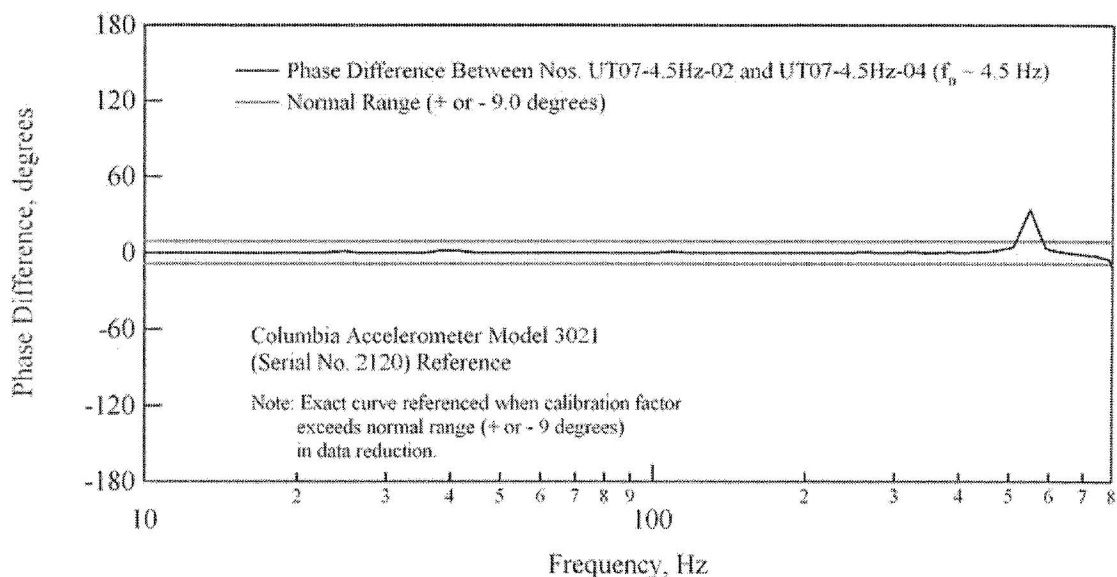


Figure AA16 Phase Difference Between GeoSpace GS-11D Geophones UT07-4.5Hz-02 and UT07-4.5Hz-04, 4.5 - Hz Resonant Frequency; Calibrated Relative to Columbia Accelerometer Model 3021 (Serial No. 2120) - 07 December 2007

**GeoSpace GS-11D Geophone Calibration – 07 December 2007**

Calibration Date : 12/07/2007

Expiration Date : 12/07/2008

Performed by : Jiabei Yuan

(Limited Calibration : Phase Only)

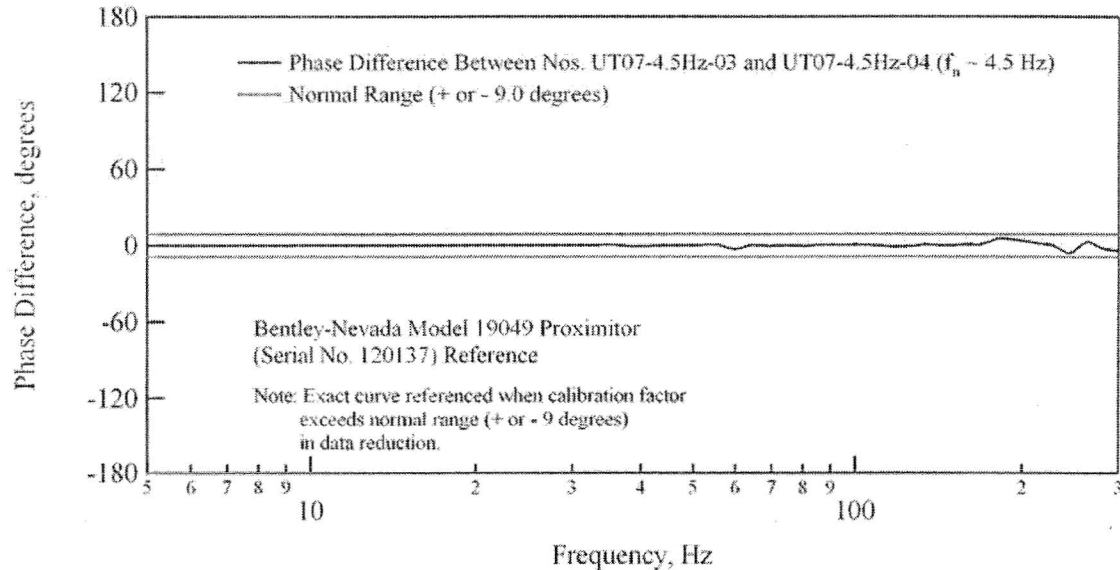


Figure AA17 Phase Difference Between GeoSpace GS-11D Geophones UT07-4.5Hz-03 and UT07-4.5Hz-04, 4.5 - Hz Resonant Frequency; Calibrated Relative to Bentley-Nevada Model 19049 Proximitor (Serial No. 120137) - 07 December 2007

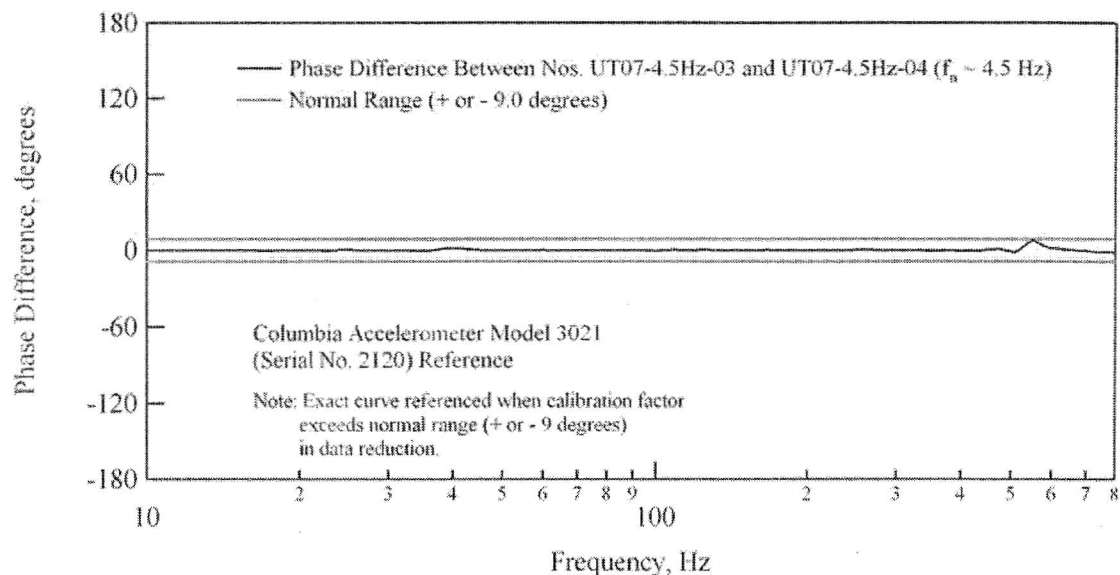
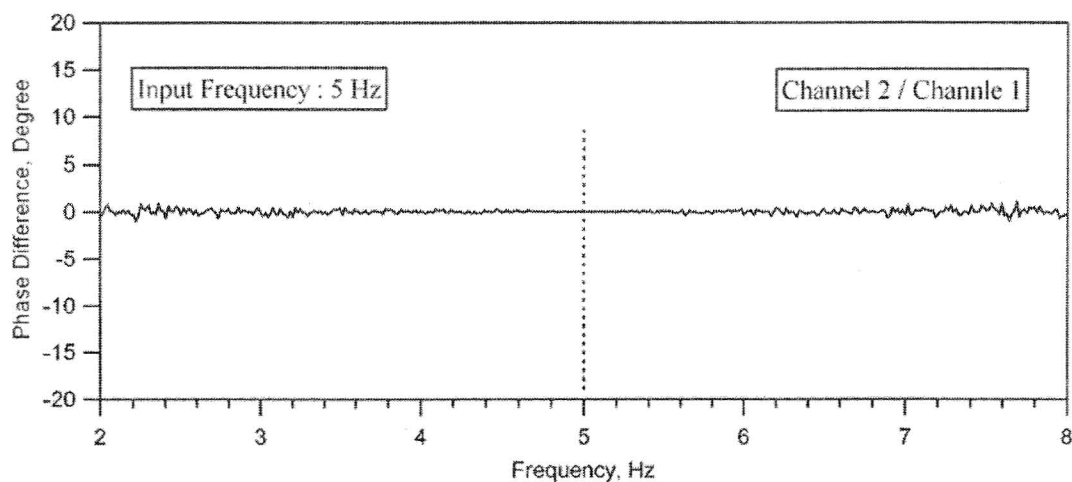
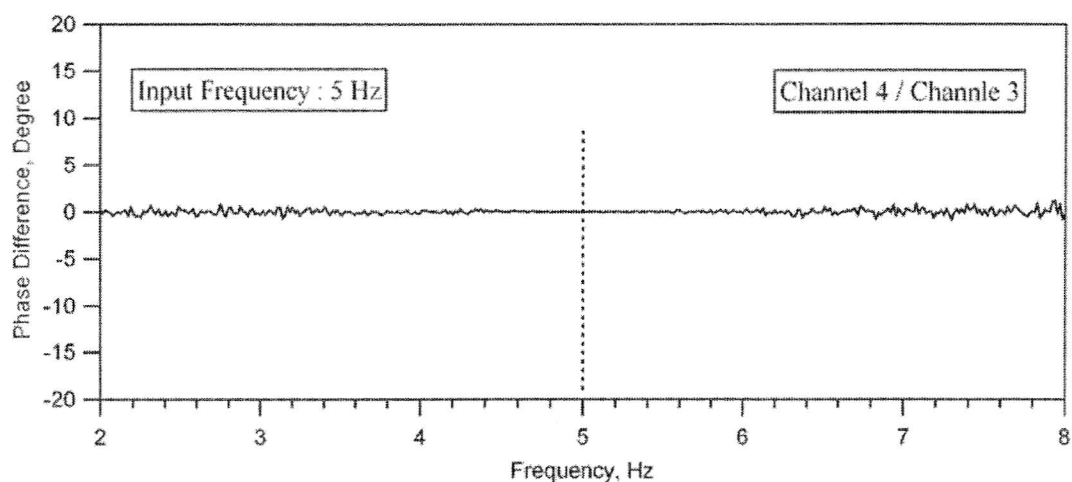


Figure AA18 Phase Difference Between GeoSpace GS-11D Geophones UT07-4.5Hz-03 and UT07-4.5Hz-04, 4.5 - Hz Resonant Frequency; Calibrated Relative to Columbia Accelerometer Model 3021 (Serial No. 2120) - 07 December 2007

# Dynamic Signal Analyzer Calibration Documentation (Frequency Domain) - (Agilent, Serial No. MY41005676)

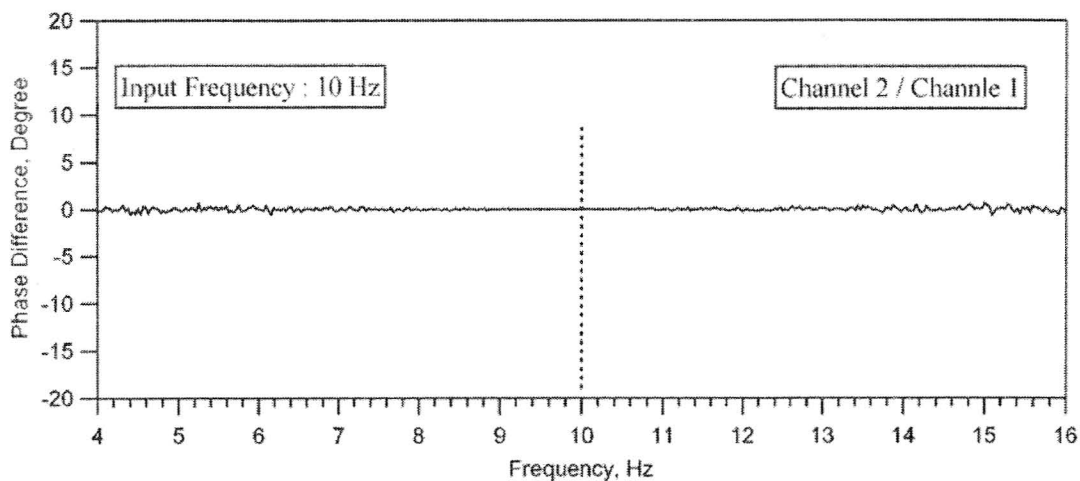


(a)

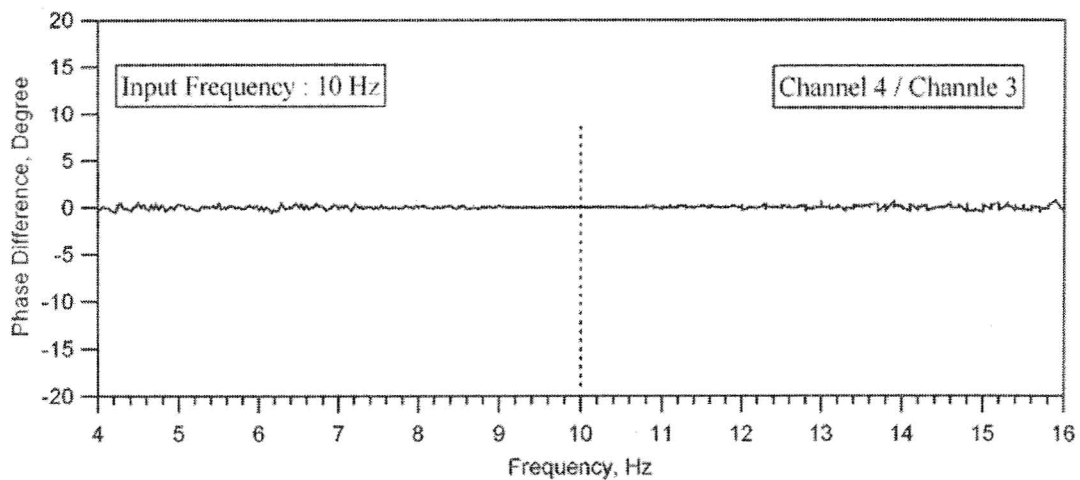


(b)

Figure AA19 Frequency Domain Calibration Records for the Agilent 4-Channel Dynamic Signal Analyzer; (a) Phase Difference Between Channel 2 and Channel 1, (b) Phase Difference Between Channel 4 and Channel 3; 5 Hz Sine Wave Input; December 10, 2007

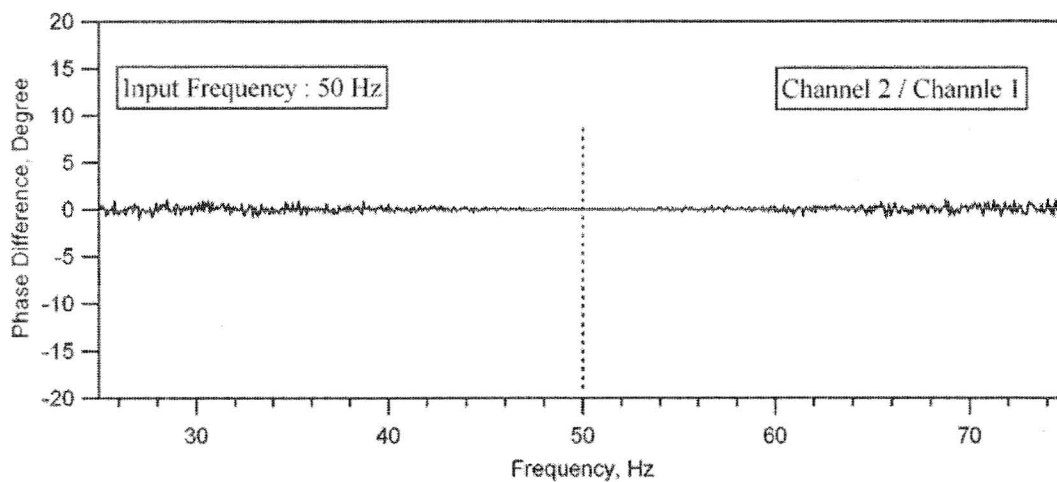


(a)

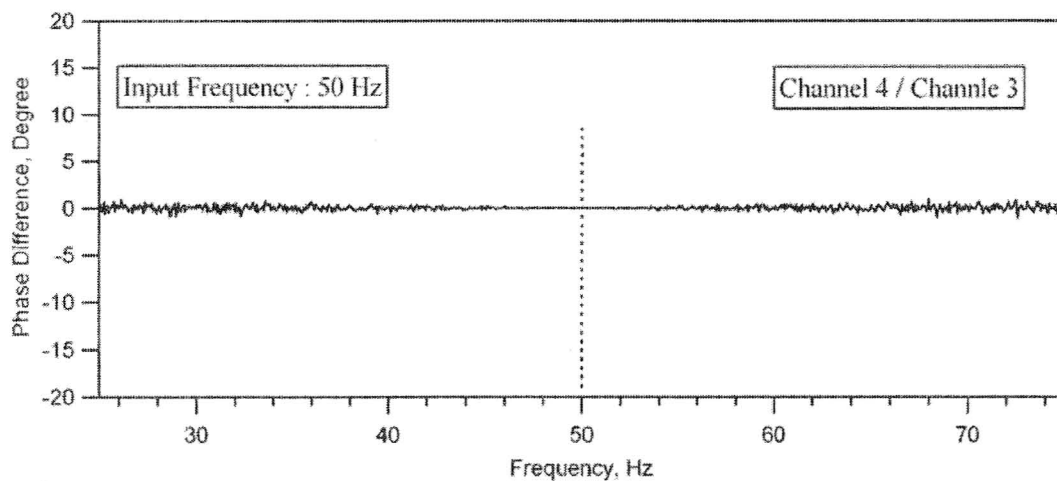


(b)

Figure AA20 Frequency Domain Calibration Records for the Agilent 4-Channel Dynamic Signal Analyzer; (a) Phase Difference Between Channel 2 and Channel 1, (b) Phase Difference Between Channel 4 and Channel 3; 10 Hz Sine Wave Input; December 10, 2007

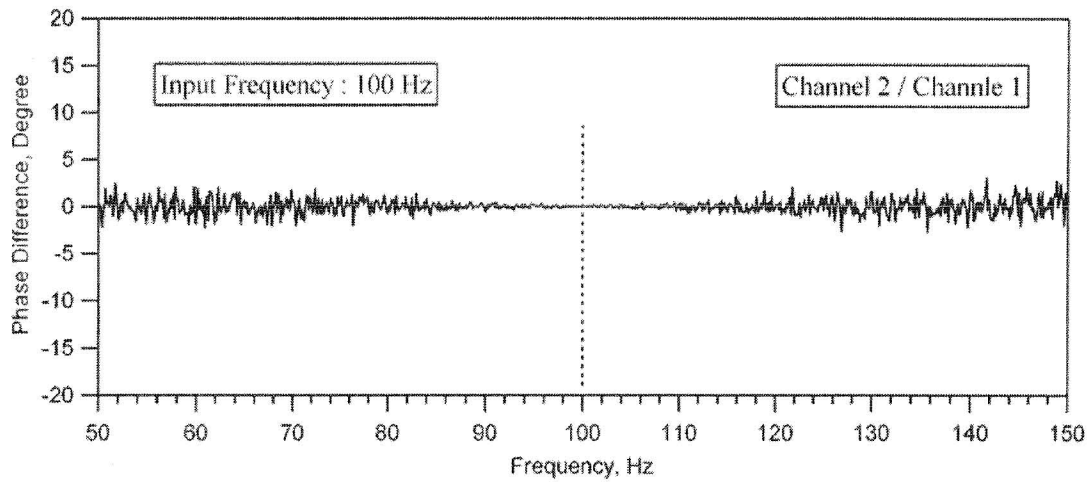


(a)

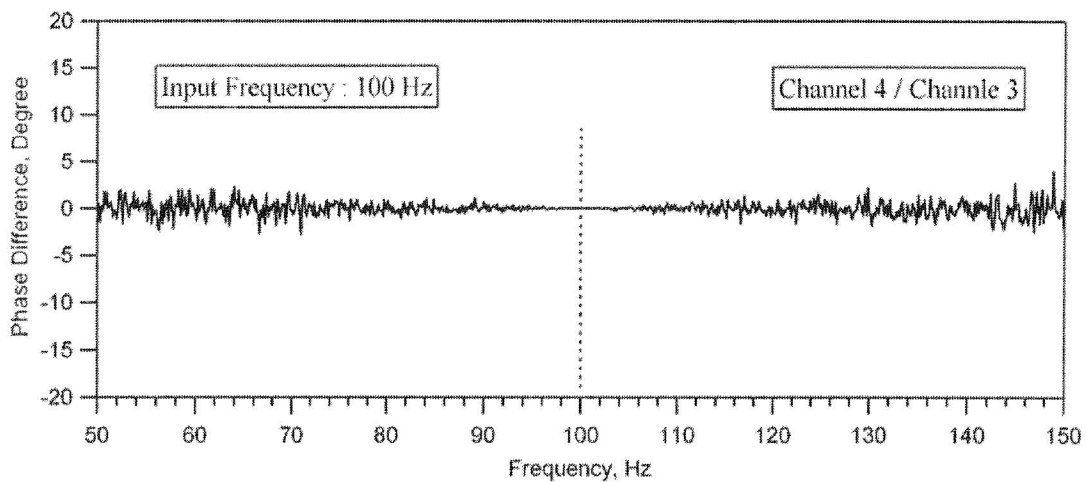


(b)

Figure AA21 Frequency Domain Calibration Records for the Agilent 4-Channel Dynamic Signal Analyzer; (a) Phase Difference Between Channel 2 and Channel 1, (b) Phase Difference Between Channel 4 and Channel 3; 50 Hz Sine Wave Input; December 10, 2007



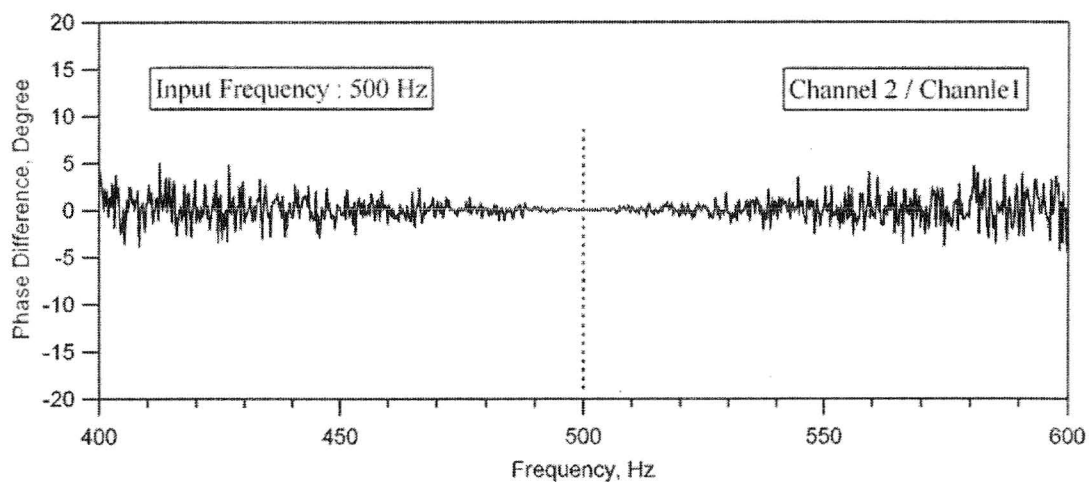
(a)



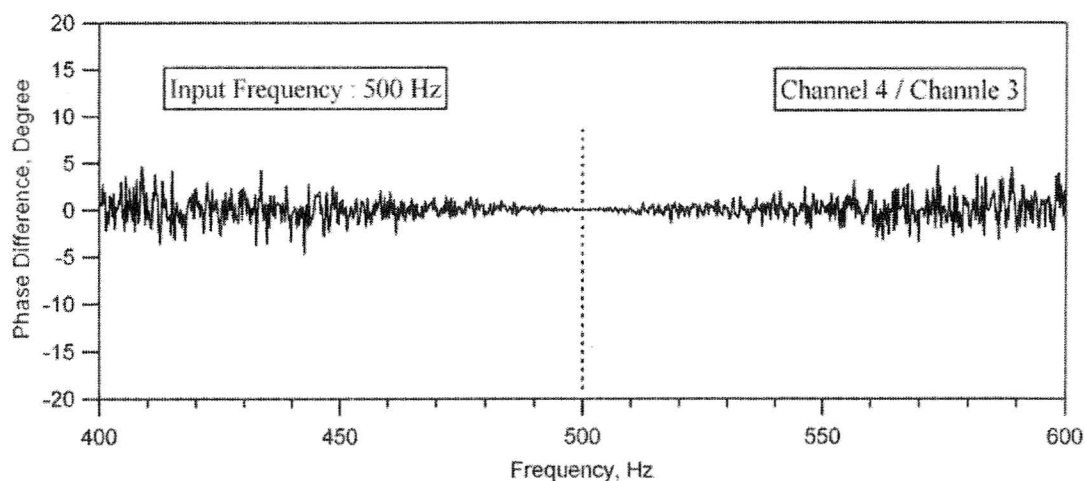
(b)

Figure AA22 Frequency Domain Calibration Records for the Agilent 4-Channel Dynamic Signal Analyzer; (a) Phase Difference Between Channel 2 and Channel 1, (b) Phase Difference Between Channel 4 and Channel 3; 100 Hz Sine Wave Input; December 10, 2007





(a)



(b)

Figure AA23 Frequency Domain Calibration Records for the Agilent 4-Channel Dynamic Signal Analyzer; (a) Phase Difference Between Channel 2 and Channel 1, (b) Phase Difference Between Channel 4 and Channel 3; 500 Hz Sine Wave Input; December 10, 2007

Table AA1 Calibration Results of Frequency Domain (Agilent Dynamic Signal Analyzer) Performed December 10, 2007

Instrument	4 Channel Dynamic Signal Analyzer Agilent, Serial No.: MY41005676		
Equipment Used	Wavetek Function Generator Model FG2A, Serial No. 912022 NIST Traceable Calibration through 5/18/2008		
Calibration Date	12/10/2007		
Input Frequency	Sine Wave 5 Hz		
Channel No.	Input Amplitude	Phase Difference	
		Expected	Measured
	V	Degree	Degree
2      1	3	0.00000	0.00020
4      3	3	0.00000	0.00083
Input Frequency	Sine Wave 10 Hz		
Channel No.	Input Amplitude	Phase Difference	
		Expected	Measured
	V	Degree	Degree
2      1	3	0.00000	0.00020
4      3	3	0.00000	0.00067
Input Frequency	Sine Wave 50 Hz		
Channel No.	Input Amplitude	Phase Difference	
		Expected	Measured
	V	Degree	Degree
2      1	3	0.00000	-0.00017
4      3	3	0.00000	-0.00064
Input Frequency	Sine Wave 100 Hz		
Channel No.	Input Amplitude	Phase Difference	
		Expected	Measured
	V	Degree	Degree
2      1	3	0.00000	0.00049
4      3	3	0.00000	-0.00022
Input Frequency	Sine Wave 500 Hz		
Channel No.	Input Amplitude	Phase Difference	
		Expected	Measured
	V	Degree	Degree
2      1	3	0.00000	0.00095
4      3	3	0.00000	0.00011

# **Appendix AB**

## **Verification of Forward Modeling Method Employed in WinSASW**

## **AB.1 INTRODUCTION**

WinSASW 1.23 (Ref. AB1) utilizes the dynamic stiffness matrix method, which was presented by Ref. AB2, to generate a theoretical phase velocity dispersion curve of surface waves generated during Spectral-Analysis-of-Surface-Wave (SASW) testing. Implementation of the Kausel-Roesset formulation was verified through comparisons of the theoretical phase velocity dispersion curves found in the scientific literature with the dispersion curves generated with WinSASW 1.23.

For the verification of the WinSASW 1.23 forward modeling routine, one comparison is shown. This comparison uses an earth profile and a corresponding theoretical phase velocity dispersion curve published in the literature (Ref. AB3).

In the following sections, the soil profile and corresponding theoretical phase velocity dispersion curve are presented. These curves are then compared with the one generated for the same profile with WinSASW 1.23.

## **AB.2 VERIFICATION THROUGH COMPARISONS**

### **AB.2.1 Comparison of WinSASW 1.23 and G.F. Panza (1980)**

The soil profile used in this comparison, which is found in “The Solution of the Inverse Problem in Geophysical Interpretation (Ref. AB3),” is shown in Figure AB1. The theoretical phase velocity dispersion curve generated by WinSASW 1.23 and the one from this article are compared in Figure AB2.

In this comparison, an excellent match between the two dispersion curves is observed. It appears that there are small differences in the low-period portion of the plot (10 to 20 seconds). One explanation for this variation is that the dispersion relation from the literature was digitized from the figure presented in the paper. However, this difference is minor and can be disregarded. Also, it should be noted, that the two-dimensional (2-D) model option in WinSASW 1.23 was used in the comparison. This model assumes plane Rayleigh waves and the fundamental mode.

$V_P = 3.8 \text{ km/s}, V_S = 2.0 \text{ km/s}, \rho = 2.2 \text{ g/cm}^3$	1 km
$V_P = 3.9 \text{ km/s}, V_S = 2.15 \text{ km/s}, \rho = 2.2 \text{ g/cm}^3$	2 km
$V_P = 4.0 \text{ km/s}, V_S = 2.3 \text{ km/s}, \rho = 2.3 \text{ g/cm}^3$	2 km
$V_P = 4.5 \text{ km/s}, V_S = 2.6 \text{ km/s}, \rho = 2.6 \text{ g/cm}^3$	9 km
$V_P = 6.1 \text{ km/s}, V_S = 3.5 \text{ km/s}, \rho = 2.7 \text{ g/cm}^3$	9 km
$V_P = 7.0 \text{ km/s}, V_S = 4.0 \text{ km/s}, \rho = 2.9 \text{ g/cm}^3$	13 km
$V_P = 8.0 \text{ km/s}, V_S = 4.4 \text{ km/s}, \rho = 3.4 \text{ g/cm}^3$	45 km
$V_P = 8.2 \text{ km/s}, V_S = 4.5 \text{ km/s}, \rho = 3.6 \text{ g/cm}^3$	290 km
$V_P = 9.0 \text{ km/s}, V_S = 4.9 \text{ km/s}, \rho = 3.7 \text{ g/cm}^3$	Half-Space

where  $V_P$  = P-wave velocity ,  
 $V_S$  = S-wave velocity, and  
 $\rho$  = mass density.

Figure AB1 Soil Profile Used in the Calculation of the Theoretical Phase Velocity Dispersion Curves Shown in Figure AB2

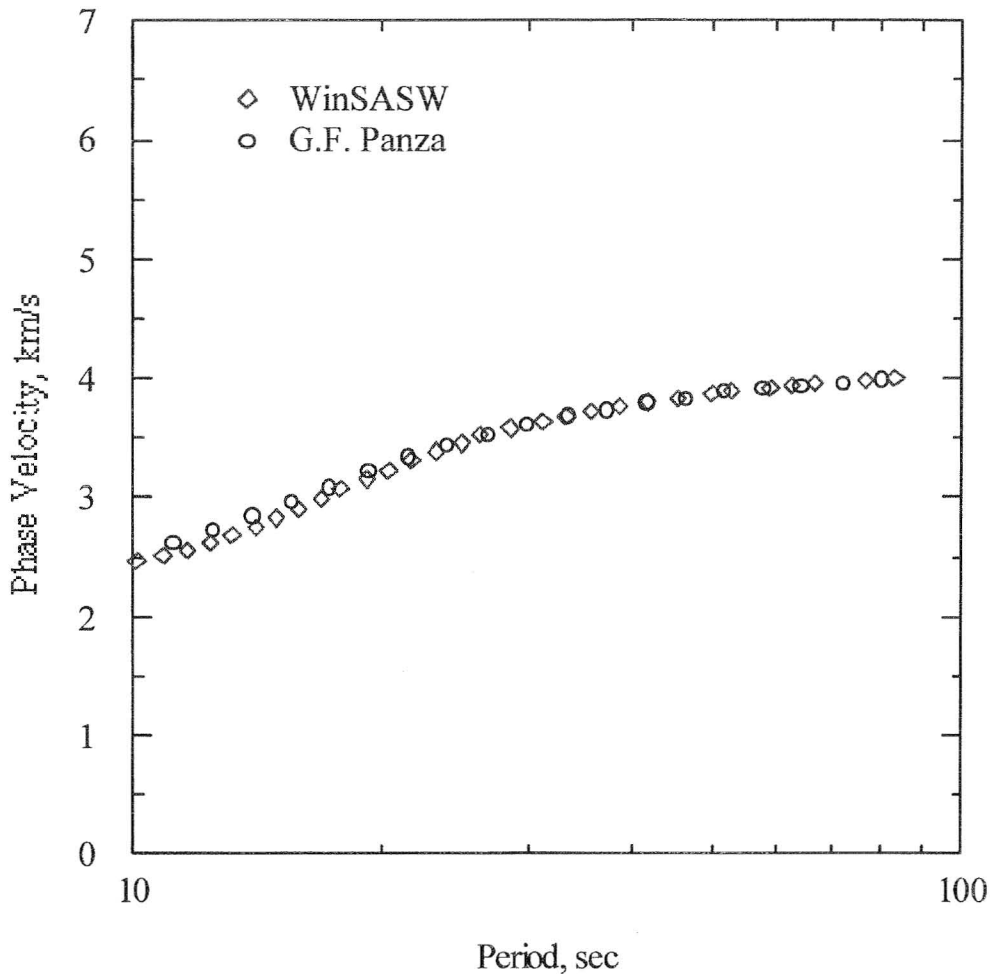


Figure AB2 Comparison of Theoretical Phase Velocity Dispersion Curves from WinSASW 1.23 and from Panza's (1980) Article

### AB.2.2 3-Dimensional Solution

The 3-dimensional model option in WinSASW 1.23 is used to analyze the SASW data collected in the field. The differences between the 2-dimensional and 3-dimensional models are not as significant as might be expected. The 2-dimensional solution models a linear wave front in a rectangular coordinate system and only includes Rayleigh-type surface waves, while the 3-dimensional solution models curved wave fronts in an axis-symmetric coordinate system. The 3-dimensional solution also includes effects of body waves. For real sites, the differences between the 2-dimensional and 3-dimensional solutions are generally not very significant. A comparison between the 2-dimensional and the 3-dimensional solutions for the soil profile shown in Figure AB1 is presented in Figure AB3. The only minor difference between these dispersion curves is at wavelengths between 30 km and 110 km that is caused by the effects of body waves

AB.4

because of the larger velocity contrast between Layer 4 ( $V_s = 2.6$  km/s) and Layer 5 ( $V_s = 3.5$  km/s).

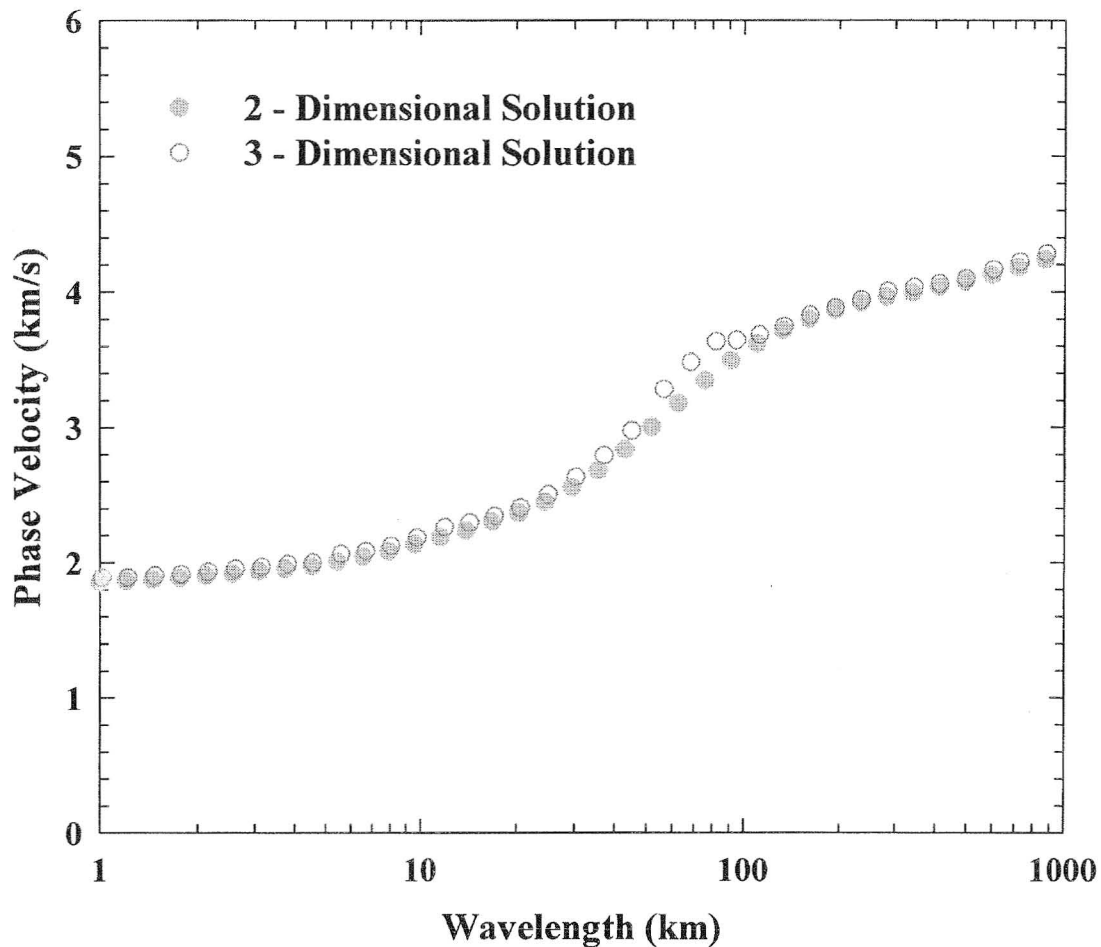


Figure AB3 Comparison Between 2-Dimensional and 3-Dimensional Dispersion Solutions Obtained from WinSASW 1.23 Using the Soil Profile Shown in Figure AB1

### AB.3 SUMMARY

Based on the comparison of the WinSASW 1.23 solution with the solution in the literature, as shown in Figure AB2, the forward modeling routine in WinSASW 1.23 is considered to be robust and reliable.

#### AB.4 REFERENCES

- AB1. Joh, S.-H., Stokoe, K.H., II, and Roesset, J.M., 1993, "WinSASW, Data Reduction and Analysis Program for SASW Measurement," Manual of Computer Program WinSASW, the University of Texas at Austin
- AB2. Kausel, C. and Roesset, J.M., 1981, "Stiffness Matrices for Layered Soils," Bulletin of the Seismological Society of America, Vol. 71, No. 6
- AB3. Panza, G.F., 1980, "The Resolving Power of Seismic Surface Waves with Respect to Crust and Upper Mantle Structural Models," in The Solution of the Inverse Problem in Geophysical Interpretation, R. Cassinis (ed.), Plenum Press, New York, 1981



# **Appendix AC**

## **Benefits and Limitations of the SASW Method**

## Benefits and Limitations of the SASW Method

The SASW method has several advantages over conventional seismic field methods in evaluating shear wave velocity profiles. First, the SASW method is both nondestructive and nonintrusive, and can therefore be performed without greatly affecting the surrounding environment. Secondly, because the SASW method does not require a borehole for the test to be performed, it can be conducted rather quickly (about 2 sites to  $V_s$ -profile depths around 500 to 800 ft per 10-hour day) and an extensive amount of ground can be investigated. This coverage is a significant advantage over borehole methods which investigate localized areas in and around the borehole. The SASW method can be a useful tool to supplement the information from borehole methods in order to fill in  $V_s$  information between boreholes. Thirdly, the SASW method is global in nature, measuring soil and rock properties over large lateral extents approximately equal to the depth of the  $V_s$  profile. Fourthly, the SASW method operates using wavelengths that are within the range of wavelengths excited by earthquakes (although they are considerably shorter than the longest wavelength excited by earthquakes). Therefore, for earthquake applications, the SASW method provides soil and rock stiffness as over a range in wavelengths that is appropriate for earthquake analysis.

Although there are several advantages gained from using the SASW method, some limitations exist that should be understood by the user of this information. First, the theoretical model used to determine the shear wave velocity profile at a site is a one-dimensional layered model, meaning there is an assumption of no lateral variation in shear wave velocity and layer thickness across the extent of the receiver array (hence uniform horizontal layers). Therefore, the profile that is presented represents a 1-D layered model that fits the measured dispersion data. It should be noted that lateral variability can be observed qualitatively from mismatches in the individual experimental dispersion curves from adjacent receiver spacings. When these cases occur, they are noted by a footnote attached to the final  $V_s$  profile and may also result in multiple interpretations and/or a reduced  $V_s$ -profile depth. Secondly, successful implementation of the SASW method requires that multiple receiver spacings are used at one site. This poses some difficulty when creating a single theoretical dispersion curve to match the experimental dispersion curve. Because the actual receiver spacing is not used, the

theoretical dispersion curve is calculated assuming that the receivers are located  $2\lambda$  and  $4\lambda$  ( $\lambda$  is wavelength) from the source. Past research has shown that this assumption does not greatly affect the final shear wave velocity profile determined at most sites.

It is important to understand that as the wavelength used in SASW testing increases, and hence the depth of penetration increases, the surface wave propagates through a greater soil volume. The resolution of the SASW method (ability to detect changes in velocity and thickness at depth) decreases as wavelength increases because larger volumes of soil are being sampled as wavelength increases. Therefore, the SASW resolution is best near the surface and decreases at greater depths in the profile. For these analyses, the shear wave velocity profiles are presented to a maximum depth of approximately 0.5 times the longest wavelength recorded in the field. The maximum profile depth is based on the fact that most of the surface wave particle motion is occurring at depths less than 0.5 times the longest wavelength. The step-wise  $V_s$  model used in the SASW analysis reflects the general trend in the shear wave velocity profile to this depth (0.5 times the longest wavelength).